Scaling of the Local Convective Heat Flux in Turbulent Rayleigh-Bénard Convection

Xiao-Dong Shang,[1,2] Penger Tong,[3] and Ke-Qing Xia[2]

[1]*Key Laboratory of Tropical Marine Environmental Dynamics, South China Sea Institute of Oceanology, Chinese Academy of Sciences, Guangzhou 510301, China*

[2]*Department of Physics, The Chinese University of Hong Kong, Shatin, Hong Kong, China*

[3]*Department of Physics, Hong Kong University of Science and Technology, Clear Water Bay, Kowloon, Hong Kong*

(Received 11 June 2007; revised manuscript received 28 April 2008; published 19 June 2008)

Local convective heat flux $\mathbf{J}(\mathbf{r})$ in turbulent thermal convection is obtained from simultaneous velocity and temperature measurements in a cylindrical cell filled with water. The measured $\mathbf{J}(\mathbf{r})$ in the bulk region shows a different scaling behavior with varying Rayleigh numbers compared with that measured in the plume-dominated regions near the sidewall and near the lower conducting plate. The local transport measurements thus allow us to disentangle boundary and bulk contributions to the total heat flux and directly check their respective scaling behavior against the theoretical predictions.

DOI: 10.1103/PhysRevLett.100.244503 PACS numbers: 47.27.te, 44.25.+f

Turbulent convection in a fluid layer confined between two horizontal plates of separation H and heated from below (Rayleigh-Bénard convection) has become an important platform to study a number of important phenomena of general interest in nonequilibrium physics [1,2]. These include the scaling of global heat transport, the dynamics of viscous and thermal boundary layers, and the interaction between a large-scale circulation (LSC) of the bulk fluid and small-scale fluctuations generated by thermal plumes. An important issue that has been under intensive experimental and theoretical scrutiny in recent years is to understand how the normalized total heat flux, which is called the Nusselt number Nu(Ra, Pr), changes with two experimental control parameters: the Rayleigh number Ra and the Prandtl number Pr [3]. Recent heat transport measurements [4] have indicated that the functional form of the measured Nu(Ra, Pr) is perhaps more complicated than simple power laws of Ra and Pr, as was originally proposed [1,2].

The theory of Grossmann and Lohse (GL) [2,5] explains this phenomenon by a decomposition of the thermal dissipation field $\epsilon_T(\mathbf{r})$ and viscous dissipation field $\epsilon_u(\mathbf{r})$ into two parts. In one scenario [2], $\epsilon_T(\mathbf{r})$ and $\epsilon_u(\mathbf{r})$ are decomposed into the boundary-layer and bulk contributions, which have different scaling behavior with varying Ra and Pr. As a result, the total heat flux measured across the entire cell contains both the boundary and bulk contributions, and thus Nu(Ra, Pr) is described by a sum of two different power laws.

Early theories [1,2] assumed that when Ra becomes very large, the bulk contribution will become dominant over the boundary-layer contribution. In this case, Nu(Ra, Pr) can be described by a simple power law of Ra and Pr. For example, Kraichnan [6] predicted an asymptotic scaling law $\mathrm{Nu} \sim (\mathrm{RaPr})^{1/2}$, which states that the convective heat flux is independent of ν and κ. The GL theory also gave the same scaling when both the thermal and viscous dissipations are bulk-dominated. While considerable experimental efforts have been made, this ultimate state of thermal convection still remains elusive [7]. This is caused partially by the fact that the boundaries are very important in this system, even when Ra becomes very large. After all, the convective flow is driven by instabilities of the upper and lower thermal boundary layers. Recent experiment [8] and numerical simulations [9] showed that the ratio of the boundary contribution of $\epsilon_T(\mathbf{r})$ to the corresponding bulk contribution is an increasing rather than a decreasing function of Ra, as was commonly believed. These studies suggest that the global heat transport measurements will always be ''contaminated'' by contributions from the boundaries.

More recently, GL proposed a second scenario [5] with $\epsilon_T(\mathbf{r})$ being decomposed into two different contributions: thermal plumes (including the boundary layers) and turbulent background. This model gives specific predictions for the local convective heat flux $\mathbf{J}(\mathbf{r})$ as a function of Ra and Pr. While the above two scenarios involve different physical pictures about the local dynamics of turbulent convection, the calculated Nu(Ra, Pr) using the two different models turns out to be of the same scaling form. This suggests that, while the GL theory is capable of providing a correct functional form of Nu(Ra, Pr) for a large number of global transport measurements [4], the microscopic mechanism of heat transport and its connection to the local dynamics still remain elusive.

In this Letter, we report direct measurements of $\mathbf{J}(\mathbf{r})$ as a function of Ra at various locations inside the convection cell. The measurements at the cell center far away from the boundaries and those measured near the sidewall and the lower conducting plate, in which the flow field is inevitably influenced by the boundaries, allow us to disentangle boundary and bulk contributions to the total heat flux and have a critical test of different theories. In the experiment, the local velocity $\mathbf{v}(\mathbf{r}, t)$ and temperature $T(\mathbf{r}, t)$ are measured simultaneously, from which we obtain the normalized local convective heat flux

$$\mathbf{J}(\mathbf{r}) = \frac{\langle \mathbf{v}(\mathbf{r}, t)\delta T(\mathbf{r}, t)\rangle_t H}{\kappa \Delta T}, \quad (1)$$

where $\delta T(\mathbf{r}, t) = T(\mathbf{r}, t) - T_0$ is the local temperature deviation from the mean temperature T_0 of the bulk fluid and $\langle \ldots \rangle_t$ represents an average over time t.

The experiment is conducted in an upright cylindrical cell filled with water. The inner diameter of the cell is $D = 19.0$ cm, and the height is $H = 19.6$ cm. So its aspect ratio is $\Gamma = D/H \simeq 1$. The upper and lower plates are made of 1-cm-thick copper, and the sidewall is a Plexiglas tube. The entire cell is placed inside a thermostat box whose temperature matches the mean temperature T_0 of the bulk fluid, which is kept at $\sim 40\,^{\circ}$C. The corresponding value of Pr is 4.4. Local velocity measurements are conducted by using a laser Doppler velocimetry system together with an argon-ion laser. Simultaneous temperature measurements are carried out by using a small movable thermistor of 0.2 mm diameter and 15 ms time constant. The mean sampling rate of the velocity measurements is ~ 25 Hz, and that of the temperature measurements is 64 Hz. Typically, we take a 20 h or longer time record ($> 2 \times 10^6$ data points) at each location, ensuring that the statistical averaging is adequate. Other details about the convection cell and heat flux measurements can be found elsewhere [10,11].

In a recent experiment [11], we measured the spatial distribution of $\mathbf{J}(\mathbf{r})$ at a fixed Ra along a cell diameter (x axis) at the midheight of the cell and along the central vertical axis (z axis) of the cell; both are in the circulation plane of the LSC. It was found that the heat flux across the midheight plane of the cell is predominately in the vertical direction. The vertical heat flux $J_z(x)$ concentrates in the plume-dominated sidewall region where the vertical velocity v_z reaches maximum [12]. The measured $\mathbf{J}(\mathbf{r})$ along the z axis is dominated by the horizontal flux $J_x(z)$ along the direction of the LSC. The measured $J_x(z)$ peaks at a location close to the edge of the thermal boundary layer. These measurements revealed that heat transport in turbulent convection is carried out mainly by thermal plumes. While the LSC provides a fast channel along the cell periphery for the transport of heat, the central region also carries heat away considerably. It is found that the bulk contribution accounts for $\sim 17\%$ of the total heat flux at $\mathrm{Ra} = 3.6 \times 10^9$ and that this percentage increases gradually with Ra.

With this spatial distribution of $\mathbf{J}(\mathbf{r})$, we now discuss the Ra dependence of $\mathbf{J}(\mathbf{r})$ at three representative locations in the cell: at the cell center, where the flow is approximately homogeneous, and near the sidewall and the center of the lower conducting surface, where the local flow is determined mainly by the LSC. Figure 1(a) shows the measured J_z at the cell center as a function of Ra. The data are well described by a power law $J_z = 3.5 \times 10^{-4}\mathrm{Ra}^{\beta}$, with $\beta = 0.49 \pm 0.03$ (solid line). This result agrees well with the GL theory for bulk-dominated dissipations [2] (same as the Kraichnan scaling [6]) and with the recent simulation results without boundary [13].

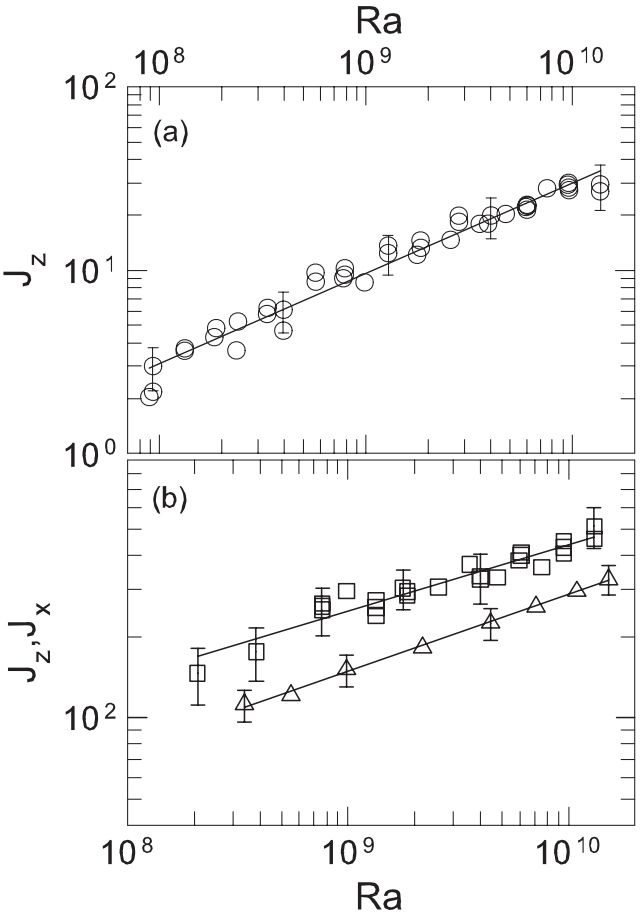

FIG. 1. (a) Measured J_z at the cell center (circles) as a function of Ra. The solid line is a power-law fit $J_z = 3.5 \times 10^{-4}\mathrm{Ra}^{0.49}$. (b) Measured J_z near the sidewall (squares) and J_x near the lower conducting plate (triangles) as a function of Ra. The solid lines are the power-law fits $J_z = 1.5\mathrm{Ra}^{0.24}$ (top) and $J_x = 0.4\mathrm{Ra}^{0.28}$ (bottom).

Figure 1(b) shows the Ra dependence of the measured J_z near the sidewall (squares) and J_x near the lower conducting plate (triangles). Because of the continuous evolution of the circulation path of the LSC, from a tilted and nearly elliptical shape at small Ra to a more squarish shape (filling out the container) at large Ra [12,14], the measurements at these two locations are conducted at a variable location (for different Ra), at which a maximal heat flux is located. The measured J_z near the sidewall is well described by the power law $J_z = 1.5\mathrm{Ra}^{\beta}$ (upper solid line), with $\beta = 0.24 \pm 0.03$. Near the lower conducting plate, we find a similar power law $J_x = 0.4\mathrm{Ra}^{\beta}$ (lower solid line), with $\beta = 0.28 \pm 0.03$. The two power-law fits give approximately the same exponent and differ only in amplitude by a factor of ~ 2.

In the second scenario of the GL theory [5], the role played by thermal plumes in determining the volume-

averaged thermal dissipation rate is considered explicitly. The new theory predicts that the local convective heat flux at the cell center has an effective power law $J_z \sim \mathrm{Ra}^{\beta}$, with $\beta \approx 0.44$ for $\mathrm{Pr} = 5.5$. Near the sidewall, the GL theory gives $J_z \sim \mathrm{Ra}^{\beta}$, with $\beta \approx 0.22$ for all Pr. The experimental results shown in Fig. 1 thus are in good agreement with these predictions. It has been shown that, in the Ra range studied here, much of the heat is transported through the sidewall region [11]. From the fitted power laws for J_z at the cell center and near the sidewall, we find that the two curves intersect at $\mathrm{Ra}_c \simeq 9 \times 10^{13}$, above which heat will be transported primarily through the central region. This finding may have important implications to large-scale astrophysical or geophysical convection, such as that in the atmosphere and oceans in which Ra can reach as high as 10^{19} [15].

To further understand the scaling results of the local heat flux, we show in Fig. 2 the Ra dependence of the characteristic local velocity v and the temperature standard deviation $\sigma = \langle [T(\mathbf{r}, t) - T_0]^2 \rangle_t^{1/2}$ at the cell center (circles), near the sidewall (squares), and near the lower conducting plate (triangles). Figure 2(a) shows the Reynolds number $\mathrm{Re} = vH/\nu$ (normalized v) as a function of Ra. At the cell center, the mean velocity is zero, and we take $v = v_{\mathrm{rms}}$, where v_{rms} is the rms value of the local vertical velocity. Near the sidewall, we take $v = \bar{v}$, where $\bar{v}$ is the mean vertical velocity, which is approximately twice larger than v_{rms} at this location [12]. Near the lower conducting plate, we use the mean horizontal velocity as v. The measured Re at the three locations can all be described by a power law $\mathrm{Re} = A\mathrm{Ra}^{\gamma}$ (solid lines). The fitted values of A and γ are given in Table I.

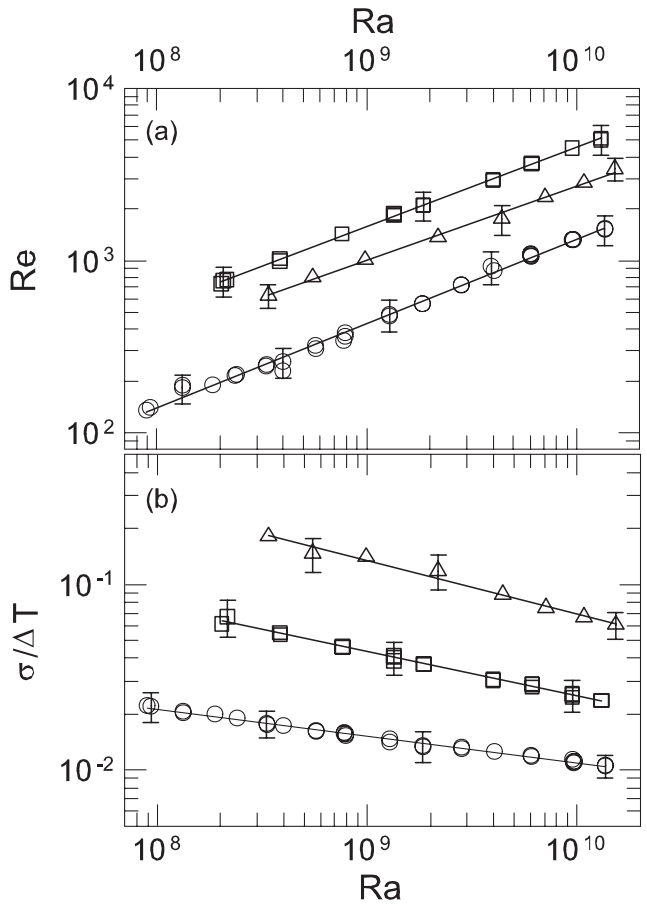

FIG. 2. (a) Measured Re at the cell center (circles), near the sidewall (squares), and near the lower conducting plate (triangles) as a function of Ra. The solid lines are the power-law fits. (b) Measured $\sigma/\Delta T$ at the cell center (circles), near the sidewall (squares), and near the lower conducting plate (triangles) as a function of Ra. The solid lines are the power-law fits.

The values of γ shown in Table I agree well with those obtained previously [12,14,16] and are close to the classical value of $1/2$ for the free-fall velocity [17]. The measured γ near the sidewall shows a small deviation from $1/2$, which is caused by a continuous evolution of the circulation path of the LSC [14]. The measured γ near the lower conducting plate has relatively larger uncertainties (± 0.04), because (i) the Ra range is smaller and (ii) the time record of the data is also shorter (6 h instead of >20 h).

Figure 2(b) shows the normalized $\sigma/\Delta T$ as a function of Ra. Similar to Re, the measured $\sigma/\Delta T$ at the three locations can also be fit to a power law $\sigma/\Delta T = A\mathrm{Ra}^{\delta}$ (solid lines), and the fitted values of A and δ are given in Table I. The value of δ at the cell center agrees well with those obtained previously [18,19]. The values of δ near the sidewall and the lower conducting plate are new results, which are approximately the same and are about twice larger than that at the cell center. Evidently, the scaling exponent δ in the plume-dominated region is larger than that in the bulk region. Figure 2(b) reveals that the amplitude of temperature fluctuations remains the largest near the lower conducting plate, becomes smaller near the sidewall, and is the smallest at the cell center. The measured δ

TABLE I. Fitted values of the power-law amplitude A and exponents for the local convective heat flux $\mathbf{J}(\mathbf{r})$, the Reynolds number Re, the normalized temperature standard deviation $\sigma/\Delta T$, and the cross-correlation coefficient C_0.

Quantity	A	Index	Value (± 0.03)
J_z (cell center)	3.5×10^{-4}	β	0.49
J_z (sidewall)	1.5		0.24
J_x (bottom plate)	0.4		0.28
Re (cell center)	1.7×10^{-2}	γ	0.49
Re (sidewall)	0.11		0.46
Re (bottom plate)	0.13		0.43
$\sigma/\Delta T$ (cell center)	0.30	δ	-0.14
$\sigma/\Delta T$ (sidewall)	5.94		-0.24
$\sigma/\Delta T$ (bottom plate)	49.5		-0.28
C_0 (cell center)	1.6×10^{-2}	ϵ	0.14
C_0 (sidewall)	0.52		0.02
C_0 (bottom plate)	1.4×10^{-2}		0.13

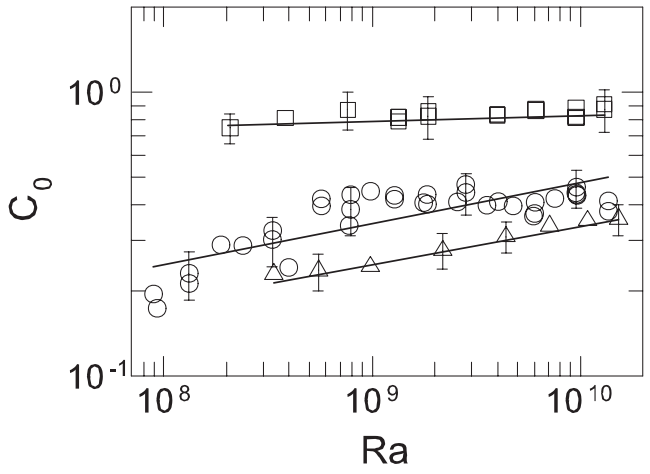

FIG. 3. Measured C_0 at the cell center (circles), near the sidewall (squares), and near the lower conducting plate (triangles) as a function of Ra. The solid lines indicate the power laws: $C_0 = 0.52\mathrm{Ra}^{0.02}$ (top), $1.6 \times 10^{-2}\mathrm{Ra}^{0.14}$ (middle), and $1.4 \times 10^{-2}\mathrm{Ra}^{0.13}$ (bottom).

at the cell center is consistent with the predicted value based on the second scenario of the GL theory [5], but in the plume-dominated region it is much larger than the theoretical value predicted for the plume-induced temperature fluctuations.

To find a relationship among the scaling exponents β, γ, and δ, we rewrite Eq. (1) as

$$J(\mathbf{r}) = C_0 \mathrm{Re} \frac{\sigma}{\Delta T} \mathrm{Pr}, \tag{2}$$

where $C_0 = \langle v(\mathbf{r}, t)\delta T(\mathbf{r}, t)\rangle_t/(v\sigma)$ is the normalized cross-correlation coefficient. In Fig. 3, we plot the directly measured C_0 at the three locations. The three solid lines are the calculated C_0 ($= J(\mathbf{r})/[\mathrm{Re}(\sigma/\Delta T)\,\mathrm{Pr}]$) using the known results of $J(\mathbf{r})$, Re, and $\sigma/\Delta T$. The obtained values of A and ϵ are given in Table I. The top and bottom lines fit the data well, but the measured C_0 at the cell center appears to saturate at $\sim$0.4 for $\mathrm{Ra} \gtrsim 10^9$, revealing some deviations from the expected power law.

The measured C_0 near the sidewall has the largest value of $\sim$0.8 and does not change much in the Ra range studied here. This result suggests that the correlation between $v(\mathbf{r}, t)$ and $\delta T(\mathbf{r}, t)$ has reached a maximal saturation value. When $v(\mathbf{r}, t)$ and $\delta T(\mathbf{r}, t)$ are fully correlated (i.e., when $C_0 \sim 1$), one may estimate the scaling exponent β by using the individually measured velocity and temperature scalings. For example, near the sidewall we have $\beta = \gamma + \delta = 0.22$, which is indeed very close to the actually measured $\beta = 0.24$ (within the experimental uncertainties). This may serve as a useful method to determine the scaling of the local heat flux in systems, where simultaneous measurement of $v(\mathbf{r}, t)$ and $\delta T(\mathbf{r}, t)$ cannot be easily made. The local horizontal velocity and temperature fluctuations near the bottom plate have the smallest correlation, but it increases with Ra as $C_0 \sim \mathrm{Ra}^{0.13}$. Because C_0 changes with Ra, the local flux scaling at the other two locations needs to be measured directly.

We have benefited from illuminating discussions with D. Lohse. This work was supported in part by NSF of China under Grants No. 10572132 and No. 40776008 (X. D. S.) and RGC of Hong Kong SAR under Grants No. CUHK403003, No. 403705 (K. Q. X.), No. HKUST-CA05/06.SC01, and No. 602907 (P. T.).

[1] E. Siggia, Annu. Rev. Fluid Mech. **26**, 137 (1994); L. P. Kadanoff, Phys. Today **54**, No. 8, 34 (2001).
[2] S. Grossmann and D. Lohse, J. Fluid Mech. **407**, 27 (2000); Phys. Rev. Lett. **86**, 3316 (2001).
[3] The Rayleigh number is defined as $\mathrm{Ra} = \alpha g \Delta T H^3/(\nu\kappa)$, where g is the gravitational acceleration, ΔT is the temperature difference across the fluid layer of height H, and α, ν, and κ are, respectively, the thermal expansion coefficient, the kinematic viscosity, and the thermal diffusivity of the convecting fluid. The Prandtl number is defined as $\mathrm{Pr} = \nu/\kappa$.
[4] X. Chavanne *et al.*, J. Fluid Mech. **557**, 411 (2006); G. Ahlers *et al.*, Phys. Rev. Lett. **86**, 3320 (2001); D. Funfschilling *et al.*, J. Fluid Mech. **536**, 145 (2005); K.-Q. Xia *et al.*, Phys. Rev. Lett. **88**, 064501 (2002); C. Sun *et al.*, J. Fluid Mech. **542**, 165 (2005).
[5] S. Grossmann and D. Lohse, Phys. Fluids **16**, 4462 (2004).
[6] R. H. Kraichnan, Phys. Fluids **5**, 1374 (1962).
[7] J. Sommeria, Nature (London) **398**, 294 (1999); J. A. Glazier *et al.*, Nature (London) **398**, 307 (1999); J. J. Niemela *et al.*, Nature (London) **404**, 837 (2000); X. Chavanne *et al.*, Phys. Rev. Lett. **79**, 3648 (1997).
[8] X.-Z. He *et al.*, Phys. Rev. Lett. **98**, 144501 (2007).
[9] R. Verzicco and R. Camussi, J. Fluid Mech. **477**, 19 (2003); R. Verzicco, Eur. Phys. J. B **35**, 133 (2003).
[10] C. Sun *et al.*, Phys. Rev. E **72**, 026302 (2005).
[11] X.-D. Shang *et al.*, Phys. Rev. Lett. **90**, 074501 (2003); Phys. Rev. E **70**, 026308 (2004).
[12] X.-L. Qiu *et al.*, Phys. Rev. E **64**, 036304 (2001).
[13] D. Lohse and F. Toschi, Phys. Rev. Lett. **90**, 034502 (2003); Phys. Fluids **17**, 055107 (2005).
[14] C. Sun *et al.*, Phys. Rev. E **72**, 067302 (2005); J. J. Niemela *et al.*, Europhys. Lett. **62**, 829 (2003).
[15] K. R. Sreenivasan and R. J. Donnelly, Adv. Appl. Mech. **37**, 239 (2001).
[16] X.-L. Qiu and P. Tong, Phys. Rev. E **66**, 026308 (2002); X.-L. Qiu *et al.*, Phys. Fluids **16**, 412 (2004).
[17] M. Sano *et al.*, Phys. Rev. A **40**, 6421 (1989).
[18] Y. Du and P. Tong, Phys. Rev. E **63**, 046303 (2001); Z. A. Daya and R. E. Ecke, Phys. Rev. Lett. **87**, 184501 (2001); Phys. Rev. E **66**, 045301 (2002).
[19] B. Castaing *et al.*, J. Fluid Mech. **204**, 1 (1989); J. J. Niemela *et al.*, Nature (London) **404**, 837 (2000); J. Fluid Mech. **557**, 411 (2006).